

GPO PRICE \$ \_\_\_\_\_

1326

CFSTI PRICE(S) \$ \_\_\_\_\_

Hard copy (HC) 2.00

Microfiche (MF) .50

# 853 July 65

ON ERRORS IN USING THE REFLECTANCE vs ANGLE OF INCIDENCE

METHOD FOR MEASURING OPTICAL CONSTANTS\*

W. R. Hunter

E. O. Hulburt Center for Space Research\*\*

U. S. Naval Research Laboratory, Washington, D. C., 20390

To be published in the  
Journal of the Optical Society of America

FACILITY FORM 802	N 66 22236	
	(ACCESSION NUMBER)	(THRU)
	28	
	(PAGES)	(CODE)
	CR-63954	23
	(NASA CR OR TMX OR AD NUMBER)	(CATEGORY)

\*Work supported in part by the National Aeronautics and Space Administration  
\*\*Sponsored jointly by the Office of Naval Research and the National Science Foundation

(1140-PRR-4/65:WRH:mgv)

~~CONFIDENTIAL~~  
~~CONFIDENTIAL~~

ON ERRORS IN USING THE REFLECTANCE vs ANGLE OF INCIDENCE  
METHOD FOR MEASURING OPTICAL CONSTANTS\*

W. R. Hunter  
E. O. Hulburt Center for Space Research\*\*  
U. S. Naval Research Laboratory, Washington, D. C., 20390

INTRODUCTION

A number of experimental methods have been devised to determine optical constants, the index of refraction,  $n$ , and the extinction coefficient,  $k$ , by means of measurements of reflectance only, without recourse to polarimetric analysis involving phase differences. Of the nine reflection methods listed by Humphreys-Owen<sup>(1)</sup>, only one is useful in all wavelength regions, since all others make some use of polarized incident radiation, which is sometimes not available, for example, in the extreme ultraviolet. This one method makes use of incident radiation which is unpolarized and is thus fairly easy to obtain. In this  $R$  vs  $\phi$  method, the reflectance,  $R$ , is measured for two, or more, angles of incidence,  $\phi$ , and the generalized Fresnel reflection equations, connecting  $R$  with  $n$ ,  $k$  and  $\phi$  are solved for  $n$  and  $k$ .

With the increased interest in optical constants, associated with solid state theory<sup>(2)</sup>, and with filter and reflector design for the extreme ultraviolet, the use of the  $R$  vs  $\phi$  method has become more common, hence it becomes

---

\*Work supported in part by the National Aeronautics and Space Administration.

\*\*Sponsored jointly by the Office of Naval Research and the National Science Foundation.

~~Not to be distributed outside of NACA Office and  
NACA Centers Only~~

important to know the limitations of the method and how it is affected by experimental errors. A brief discussion of errors was given by Humphreys-Owen and by Collins and Bock<sup>(3)</sup>; however, no systematic study of the errors involved has been published, probably because this cannot be done analytically, and it is necessary to resort to numerical computation. The use of high speed digital computers has reduced the time required for such computations by orders of magnitude and made possible the present study of the sensitivity of, and the effect of errors on the  $R$  vs  $\phi$  method. Although undertaken in connection with an investigation of the optical properties of materials in the extreme ultraviolet, the study was broadened to include the reflectances  $R_s$  and  $R_p$  for incident radiation polarized with the electric vector perpendicular, and parallel, respectively, to the plane of incidence.

#### GENERAL DISCUSSION OF THE $R$ vs $\phi$ METHOD

The method is based on the premise that any  $R$  vs  $\phi$  curve, in the absence of interference effects, is uniquely determined by the pair of constants  $n$  and  $k$  which are related to the reflectance by the generalized Fresnel reflection equations:

$$R_s = [(a - \cos \phi)^2 + b^2] / [(a + \cos \phi)^2 + b^2]$$

$$R_p = R_s \cdot [(a - \sin \phi \tan \phi)^2 + b^2] / [(a + \sin \phi \tan \phi)^2 + b^2]$$

$$R_a = \frac{1}{2} (R_p (1 + p) + R_s (1 - p))$$

where

$$a^2 = \frac{1}{2} \left\{ \left[ (n^2 - k^2 - \sin^2 \phi)^2 + 4n^2 k^2 \right]^{\frac{1}{2}} + (n^2 - k^2 - \sin^2 \phi) \right\}$$

$$b^2 = \frac{1}{2} \left\{ \left[ (n^2 - k^2 - \sin^2 \phi)^2 + 4n^2 k^2 \right]^{\frac{1}{2}} - (n^2 - k^2 - \sin^2 \phi) \right\}$$

and  $p$  is the polarization. Since these equations cannot be solved explicitly for  $n$  and  $k$ , various means have been devised to obtain the solution<sup>(4, 5, 6, 7, 8)</sup>; however, all are essentially the same since they represent simultaneous solutions of the Fresnel equations and involve a graphical procedure. Hence, the results presented in this paper apply to all of these methods.

One manner in which the method is used is shown in Fig. 1. The curves on the left side of the figure, show  $R$  as a function of  $n$  for constant values of  $k$ , for a particular angle of incidence, in this case  $20^\circ$ . Suppose that the measured value of  $R$  for  $20^\circ$  is 30%, shown by the heavy horizontal line. This value of  $R$  corresponds to many pairs of  $n$  and  $k$ , which when plotted in the  $n$ - $k$  plane on the right side of the figure, give the isoreflectance curve for  $20^\circ$ , shown by the heavy line labelled  $20^\circ$ . Similarly a reflectance measurement at another angle of incidence would provide a second isoreflectance curve, and the intersection with the first curve would be the solution for  $n$  and  $k$ . In practice, it is best to measure the reflectance at more than two angles of incidence, and there is seldom a common point of intersection, as is illustrated on the right. When such is the case the center of gravity, CG, of the figure formed by the intersecting curves is taken as the solution. A separate calculation should then be performed to verify that the CG is indeed the best fit.

The spread of intersections may be caused by errors in measuring  $R$ ,  $\phi$ , by a small amount of polarization of the incident radiation, by the presence of surface layers or a combination of these effects. The net result is reflectance values inconsistent with those that would be calculated using the Fresnel equations. Hence the isorefectance curves will not have a common intersection.

#### THE SENSITIVITY OF THE METHOD

A measure of the sensitivity of the method is the angle of intersection of the isorefectance curves since this is the factor that determines the change in location of the intersection for a given error in the measurement. If the angle is small, a slight displacement of the isorefectance curves will cause a large shift in the position of the intersection, while for an angle of intersection of  $90^\circ$ , the shift is minimized and the maximum accuracy is obtained.

The sensitivity of the method was examined by plotting isorefectance curves derived from reflectance values calculated from the Fresnel equations. A digital computer was programmed to trace the isorefectance curves with the aid of a plotter rather than use the graphical method illustrated in Fig. 1 and have the data suffer cumulative errors in going through the necessary steps. The scheme for obtaining isorefectance curves via the computer-plotter combination is presented in the appendix along with a short discussion of the accuracy involved.

Since the sensitivity of the method is dependent on  $n$  and  $k$ , hence on the shape of the  $R$  vs  $\phi$  curves, these curves are shown in Fig. 2 for reference during the ensuing discussions of sensitivity and error. The large

numbers give the values of  $n$  and  $k$  used in calculating the particular set of curves while the smaller numbers along the ordinate axis show the percent reflectance and those along the abscissal axis show the angle of incidence. In each square, the upper curve is the perpendicular component,  $R_s$ , the lower curve is the parallel component,  $R_p$ , and the center curve is the arithmetic average of the two,  $R_a$ . With the exception of the lower left hand square,  $n = 0.3$ ,  $k = 0.3$ , the  $R_s$  curves are all monotonic in character. The  $R_a$  curves are also, except for the large values of  $n$  and  $k$  where a slight minimum can be seen. Also, for large  $n$  and  $k$ , the  $R_a$  curves are approximately constant from normal incidence to fairly high angles, for example, for  $n = 2.3$  and  $k = 2.3$ ,  $R_a$  is constant from normal incidence to approximately  $65^\circ$ . The  $R_p$  curves all have definite minima, and a point of inflection located between minimum reflectance and normal incidence.

The isorefectance curves for  $R_s$  are shown in Fig. 3. Eight angles of incidence are shown, from  $10^\circ$  through  $80^\circ$ , with intervals of  $10^\circ$ . The number 8 indicates the isorefectance curve for  $80^\circ$  angle of incidence and the other curves occur in descending order,  $70^\circ$ ,  $60^\circ$ , etc., to  $10^\circ$ . The same order occurs in all cases. Maximum sensitivity is obtained for small  $n$  and  $k$ , otherwise the angles of intersection are so small that accurate results would be impossible to obtain. A slight error in the measurement of reflectance, whatever the cause, would result in a large displacement of the point of intersection. For example, for  $n = 0.3$ , and  $k \geq 1.3$ , displacements will cause large errors in  $k$  which will increase as  $k$  increases.

On the other hand, for  $n = 1.8$  and  $k = 1.3$ , displacements will cause large errors in  $n$ . Thus, use of the perpendicular component is a very insensitive method for obtaining  $n$  and  $k$  and it will not be considered further.

In Fig. 4, are shown isorefectance curves for  $R_p$ . Once again eight angles of incidence are shown from  $80^\circ$  through  $10^\circ$  at intervals of  $10^\circ$ . The  $80^\circ$  curve is designated by the number 8 and, where necessary, the other angles are similarly designated by a single digit. The angles of intersection are larger than those shown for  $R_s$  indicating that use of the parallel component for obtaining  $n$  and  $k$  is a more sensitive method. The region of least sensitivity occurs for small  $n$  and  $k \geq 1.3$ . Here the angles of intersection are still small enough so that appreciable errors in  $k$  can be caused by small errors in the measurement of reflectance, however, as  $n$  increases, the angles of intersection increase causing an increase in sensitivity.

There are three unusual features associated with the  $R_p$  curves which will be pointed out briefly. First, the order in which the curves occur is not always the same as for the perpendicular component. For example, for  $n = 0.8$  and  $k = 0.3$ , there is a reversal of order at approximately  $30^\circ$  angle of incidence. For larger values of  $k$  the reversal still occurs but at smaller angles of incidence where the curves are so close together that it cannot be seen in this figure. The square corresponding to  $n = 1.3$  and  $k = 0.3$  is a good example of a reversal at the smaller angles where the isorefectance curves are in close proximity. Note that the curves for  $40^\circ$  and  $10^\circ$  coincide as do the curves for  $30^\circ$  and  $20^\circ$ . The physical reason

For this reversal is not known. At first it was thought to be associated with the point of inflection in the  $R_p$  vs  $\phi$  curves but for  $n = 2.3$  and  $k = 0.3$ , the inflection point occurs between  $50^\circ$  and  $60^\circ$  while the reversal of order occurs at angles less than  $30^\circ$ . The second feature is most easily seen in the two lower right squares,  $k = 0.3$  and  $n = 2.3$  and  $1.8$ . The rate of change in angle of intersection with angle of incidence has a maximum at approximately  $60^\circ$  for  $n = 1.8$  and at approximately  $65^\circ$  for  $n = 2.3$ . Careful inspection has shown that this effect is present for all  $n$  and  $k$  shown in the figure although it is not easily seen for small  $n$  because it occurs between  $70^\circ$  and  $90^\circ$ . The angle of incidence at which the maximum rate of change of intersection angle occurs is the principal angle of incidence,  $\bar{\phi}$ , that is, the angle of incidence where the phase difference between  $R_s$  and  $R_p$  is  $90^\circ$ . This angle practically coincides with the angle of incidence at which minimum reflectance occurs, however, the two angles should not be confused for as  $k$  increases,  $\bar{\phi}$  occurs at larger angles than  $R_p$  (min) although the separation for these values of  $n$  and  $k$  is never more than a few degrees. In principle, maximum accuracy can be obtained by using reflectance measurements around this angle of incidence since the angle of intersection could be close to  $90^\circ$ , however, referring to Fig. 1, it is seen that  $R_p$  has a very small value for  $k < 2.3$  in the region of  $\bar{\phi}$ , for example, if  $n = 2.3$  and  $k = 0.3$ ,  $R_p(\bar{\phi}) < 1\%$ , so the increase in accuracy due to the optimum intersection may be cancelled by the errors in measuring such small reflectance values.

Third, in the square corresponding to  $n = 1.8$  and  $k = 0.3$ , there are multiple intersections of the  $60^\circ$ ,  $70^\circ$ , and  $80^\circ$  isoreflexance curves.



The fact that these curves have three distinct intersections does not belie the premise that each reflectance vs angle of incidence curve is uniquely determined by one pair of  $n$  and  $k$ , rather it means that the reflectance at, say  $70^\circ$  and  $80^\circ$  angle of incidence, can be the same for more than one pair of  $n$  and  $k$ . This was the only example of multiple intersections found during the course of this work, and the ambiguity that it introduces is dispelled by the intersections of the isorefectance curves for smaller angles of incidence that show which intersection is the correct one.

Figure 6 shows isorefectance curves for  $R_a$ . The angles of intersection are smaller than for  $R_p$  and larger than for  $R_s$ . There is no reversal of order nor did any multiple intersections appear. It is worth noting that for  $n > 1.3$ , the angles of intersection tend to be small for angles of incidence  $< 80^\circ$ . Thus, if possible, it is worthwhile including reflectance measurements in the angular region of  $80^\circ$ , providing they can be accurately made, to increase the sensitivity, otherwise large errors may result because of the small intersection angles.

The isorefectance curves show that the use of  $R_p$  gives greatest sensitivity for obtaining  $n$  and  $k$ ,  $R_s$  is virtually useless and  $R_a$  gives a sensitivity between the two. For  $R_a$  it is generally the case that greater sensitivity is obtained at angles of incidence where the reflectance is changing most rapidly, however, an exception occurs for  $n \leq 0.8$  and  $k = 0.3$  where  $70^\circ$  and  $80^\circ$  isorefectance curves have the smallest angle of intersection.

Maximum sensitivity for the parallel component is obtained in the region of the principal angle of incidence, however, for  $k > 0.3$ , this angle occurs at large angles of incidence,  $> 60^\circ$ , so that the general conclusion drawn for  $R_s$  may be said to apply to  $R_p$  as well provided  $k$  is not too small.

#### EFFECT OF ERRORS ON THE DETERMINATION OF $n$ AND $k$

The effect of errors can be determined by altering the calculated reflectance data suitably and plotting the isorefectance curves corresponding to the imperfect data via the computer-plotter combination. If there is an error in  $R$ , the isorefectance curve will be shifted along its normal by an amount depending on the magnitude of the error and in a direction depending on its sign. Consequently, if isorefectance curves for both positive and negative errors are plotted, an area of intersection, such as that shown in Fig. 6 for the  $20^\circ$  and  $70^\circ$  curves, is obtained. A complete error study for all eight angles of incidence could not be presented since the inclusion of twelve curves would be quite confusing. For this reason, and because most of the published curves<sup>(5,6)</sup> used to obtain  $n$  and  $k$  were calculated for only two angles of incidence, namely  $20^\circ$  and  $70^\circ$ , these two angles were chosen to show the effects of errors.

In Fig. 7 is shown the effect of non-parallelism of the incident radiation; the divergence of the beam was taken as  $4^\circ$  which is approximately the case for full grating illumination with a 1 meter radius of curvature, normal incidence monochromator. The reflectance value was obtained by averaging the calculated reflectance over 10 angles of incidence equally spaced on either side of the chosen angle. For example, the reflectance at  $70^\circ$  was the average

of the reflectance from  $68^\circ$  through  $72^\circ$  taken every  $0.2^\circ$ . Since the sign can be only plus or minus in this case, there are no four-sided figures. The averaging procedure tacitly assumes that the emergent beam from the monochromator is uniform. If this is not the case, farther corrections must be made. The errors, shown by the departure of the heavy lines from the grid lines, are small and are confined to the lower right hand side of each figure, that is, for large  $n$  and small  $k$ . The p-component is slightly more tolerant of non-parallelism than the average.

Figure 8 shows the effect of  $\pm 1\%$  error in measuring  $R_a$  or  $R_s$ . In this case the four-sided areas of intersection filled in with black, together with the lines connecting the extremities of these areas, indicate the errors to be expected in  $n$  and  $k$ . For  $n = 0.3$ , the error in  $n$  does not increase as rapidly with increasing  $k$  as does the error in  $k$  because the isorefectance curves for  $n = 0.3$  and  $k \geq 1.3$  were almost parallel to the  $k$  axis, as shown in Figs. 4 and 5, and had small intersection angles, hence a small error in reflectance causes a large displacement of the intersection in the  $k$  direction. As  $n$  increases, and for large  $k$ , the long axis of the intersection figure rotates so that the error in determining  $n$  increases while that for  $k$  decreases. If  $80^\circ$  had been chosen for the large angle of incidence rather than  $70^\circ$ , the errors would have been smaller for  $R_a$ , especially for large  $n$ , since the  $80^\circ$  isorefectance curve showed a much larger angle of intersection with the  $20^\circ$  isorefectance curve. This generally holds

for  $R_p$  with the exception of  $k = 1.5$  and  $n = 2.3$  and  $1.8$ . Here the angle of intersection of the  $80^\circ$  and  $20^\circ$  curves has exceeded  $90^\circ$  and approaches  $180^\circ$ , hence  $70^\circ$  is the better choice. Once again it can be seen that the p-component is more tolerant of errors than  $R_a$ .

Errors caused by a small amount of polarization in the incident radiation used in measuring  $R_a$  are shown in Fig. 9. Because the polarization has very little effect at  $20^\circ$  angle of incidence, and a large effect at  $70^\circ$ , the regions of intersection appear to be lines on the scale in this figure, although on the original plot they have four sides. The solid and dotted lines connecting the extremities of the intersection figures indicate the magnitude of errors for  $\pm 1\%$  and  $\pm 5\%$  polarization, respectively. Minimum error occurs for small  $n$  and  $k$  and increases as both  $n$  and  $k$  increase.

#### ALTERNATIVE METHOD OF OBTAINING $n$ AND $k$ FROM REFLECTANCE MEASUREMENTS

The computer program used to plot the isorefectance curves from calculated data can also be used to obtain  $n$  and  $k$  from experimental data. There are two disadvantages to this scheme, however; first, the best fit must still be determined once the intersections of the isorefectance curves have been plotted, and second, corrections for polarization of the incident radiation cannot easily be made.

Figure 10 illustrates an alternate scheme, suitable for digital computation, that can be corrected for polarization of the incident radiation. The formula in the figure is that for a least squares fit which is obtained by varying the parameters  $n$ ,  $k$ , and the polarization  $p$ . The calculation proceeds as

follows: An arbitrary value for  $p$  is assigned, a point in the  $n-k$  plane, designated by the subscript  $j$ , is chosen and for each angle of incidence, designated by the subscript  $i$ , the square of the difference between the measured and calculated reflectance is determined. These differences are then summed over the desired angles of incidence, giving a number,  $M_j(p)$ , that is the least square error in fitting the experimental curve with the one obtained from the trio of parameters  $n$ ,  $k$ , and  $p$ . The computation proceeds from an initial point,  $j = 0$ , shown in the figure by  $n_0$ ,  $k_0$ . Eight additional pairs of  $n$  and  $k$ , corresponding to the eight points shown on the perimeter of the square, are generated, and  $M_j(p)$  calculated for each point. The order of numbering is unimportant. Each point is tested to find the minimum  $M(p)$  among the nine points, the center of the square is moved to that point and the procedure repeated. The small arrows indicate a possible path that will be followed by the square for a constant value of the parameter  $p$ , and the heavy lines represent constant least square error contours, or curves of constant  $M(p)$ . When finally the center point is the minimum, the data has been fitted by least squares with the error  $M_0(p)$ . A new value for  $p$  is chosen and the entire calculation repeated. In this manner the best fit to the experimental curve is obtained and the final values of the parameters give the desired values for  $n$ ,  $k$ , and also the polarization of the radiation emerging from the monochromator.

The least squares method does not require a knowledge of the absolute reflectance values. However, if relative reflectance values are used, it will

be necessary to normalize the experimental  $R$  vs  $\phi$  curve and all calculated reflectance values at some angle of incidence.

## APPENDIX

The problem of tracing an isorefectance curve in the  $n - k$  plane for a given  $\phi$  is that of finding the locus of points corresponding to a given reflectance,  $R(g)$ . Since the Fresnel equations cannot be solved explicitly for  $n$  and  $k$  in terms of  $R$  and  $\phi$ , the points of the locus must be found one by one by comparing the reflectance calculated at a particular point,  $R(c)$ , with  $R(g)$  and changing  $n$  and  $k$  until this difference is less than a predetermined error. The accuracy with which the isorefectance curve will be traced depends on the accuracy with which  $R(c)$  and  $R(g)$  are matched.

If there is no a priori knowledge of  $n$  and  $k$ , the computation must start at some arbitrary point in the  $n - k$  plane. Since isorefectance curves start and end on the  $n$  axis, it is most convenient to start at the origin and move along the  $n$  axis in small steps, comparing  $R(c)$  and  $R(g)$  until the difference between the two is equal to, or less than the specified error. This point becomes the initial point and the computation then proceeds in the following manner.

An array of eleven points, each designated by a subscript  $j$ , is generated in the  $n - k$  plane according to the diagram on the left of Fig. 11, where points 9, 10, and 11 are identical to points 1, 2, and 3. During computation only five adjacent points, operational points, are used at a time to ensure that the tracing

always proceeds in the same direction. It is convenient to have an indexing number,  $m$ , that runs from 1 through 5, to keep track of these points and so that no manipulations are done with the subscripts  $j$ . Thus the five values assigned to  $m$  correspond to certain sets of five  $j$  values.

Once the eleven points have been obtained, five operational points must be chosen for the tracing. Their selection depends on the direction in which the tracing is to proceed. Suppose the isorefectance curve shown to the right in Fig. 11 is to be traced, beginning on the  $n$  axis at position 1. In this position,  $m$  goes from 1 through 5, as does  $j$ , and the uppermost five points, shown by the heavy dots, are used. After choosing these points, the absolute value of the difference between  $R_j(c)$  and  $R(g)$ ,  $N_j$ , is calculated and the minimum and next largest  $N$  determined. When these two points have been obtained, the difference between  $R_j(c)$  and  $R(g)$  is calculated for each of them and a linear interpolation performed to obtain the point corresponding most closely to  $R(g)$ . This point becomes the new position for the array center, and the plotter, in tracing the movements of the array center, traces the isorefectance curve.

As the array moves along the isorefectance curve, a point will eventually be reached at which the isorefectance curve goes between the points  $m = 4$  and 5, ( $j = 4$  and 5). When this happens, the array center is not shifted; instead  $m$  is replaced by  $m + 2$  so that the five new points, which correspond to  $j = 6$  through 7, are arranged as shown by the heavy dots in position 2, after which the calculation proceeds as usual. This position is maintained

until the isoreflectance curve again passes between  $m = 4$  and  $5$ , ( $j = 6$  and  $7$ ) when  $m + 2$  is replaced by  $m + 4$  and the orientation is shown in position 3, and so on. If the isoreflectance curve should curve in the opposite direction, a similar procedure is used when it passes between  $m = 1$  and  $2$ ; however, when the array goes from position 1 to position 4,  $m$  is replaced by  $m + 6$  and not  $m - 2$ , and if the curvature does not change sign, eventually  $m + 6$  will be replaced by  $m + 4$ , etc.

The Naval Research Laboratory program is set up so that corresponding pairs of  $\phi$  and  $R$  are entered as data. Tracing for a particular pair of  $\phi$  and  $R$  is terminated when  $n$  or  $k$  go beyond predetermined boundaries, at which time a new pair of  $\phi$  and  $R$  are taken from storage and the next isoreflectance curve traced.

The computation need not start at the origin but can be started at any convenient point in the  $n - k$  plane. Provision should also be made for moving along the  $k$  axis to find the initial point because, if the tracing is to be restricted to a small portion of the  $n - k$  plane, the isoreflectance curves may not intersect the  $n$  axis. For example, in Fig. 5, the square for  $n = 2.3$ ,  $k = 1.3$ , it was necessary to move along the  $k$  axis to find the initial point. In this case, the initial  $m$  was  $m + 2$ , since the initial position was position 2.

The greatest possibility for error occurs in the linear interpolation to find the new position for the array center. Other interpolation schemes may



be used, of course, but the error in using a linear interpolation is quite small judging by the intersections obtained in Figs. 3, 4, and 5. The originals of these curves were traced on  $15.24 \times 15.24$  cm squares with a scale of 0.254/cm for both  $n$  and  $k$ . The size of the array was  $0.05 \times 0.05$  cm, which means that the array center movement was between 0.025 and 0.035 cm. The intersections were point-like to within the width of the line traced by the pen which was less than 0.025 cm.

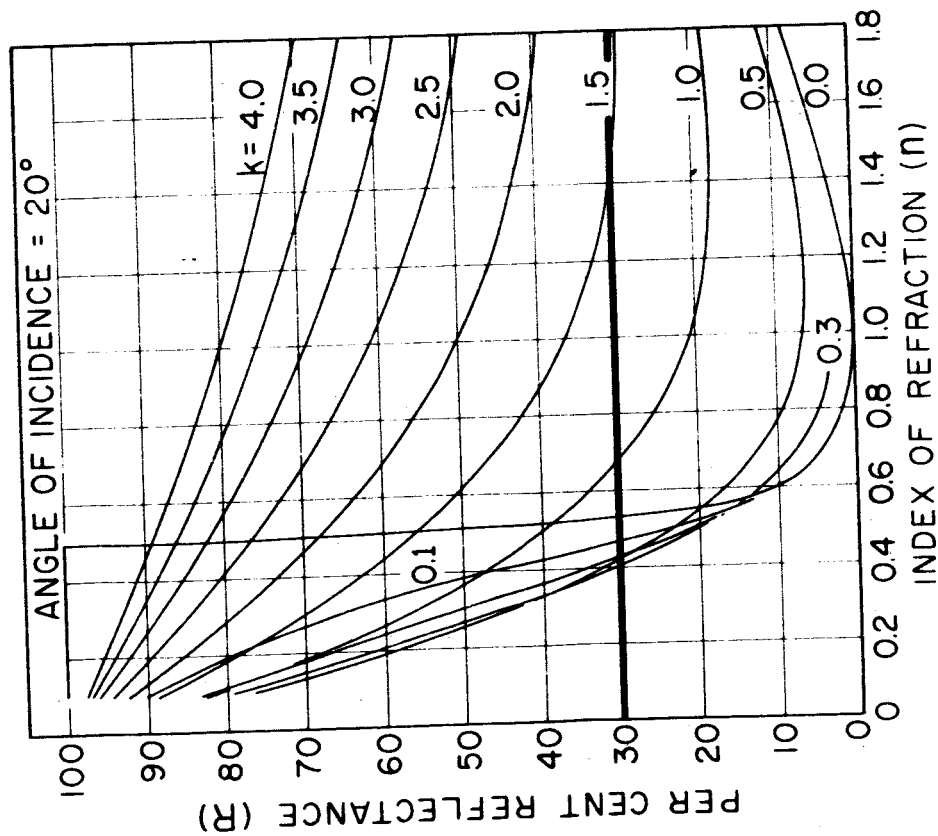
#### REFERENCES

1. S. P. F. Humphreys-Owen, Proc. Phys. Soc. 77, 949, 1961.
2. J. C. Phillips, Phys. Rev. 133, A452, 1964.
3. J. R. Collins and R. O. Bock, Rev. Sci. Inst. 14, 135, 1943.
4. R. Fousey, J. Opt. Soc. Am. 29, 235, 1939.
5. I. Simon, J. Opt. Soc. Am. 41, 336, 1951.
6. P. Sasaki and K. Ishiguro, Japanese J. of Appl. Phys. 2, 289, 1963.
7. P. W. Baumeister, Private communication.
8. A. Vasicsek, "Tables of Determination of Optical Constants from the Intensities of Reflected Light," Publ: Nakladatelstvi Ceskoslovenske Akademie Vec, Prague (1964).

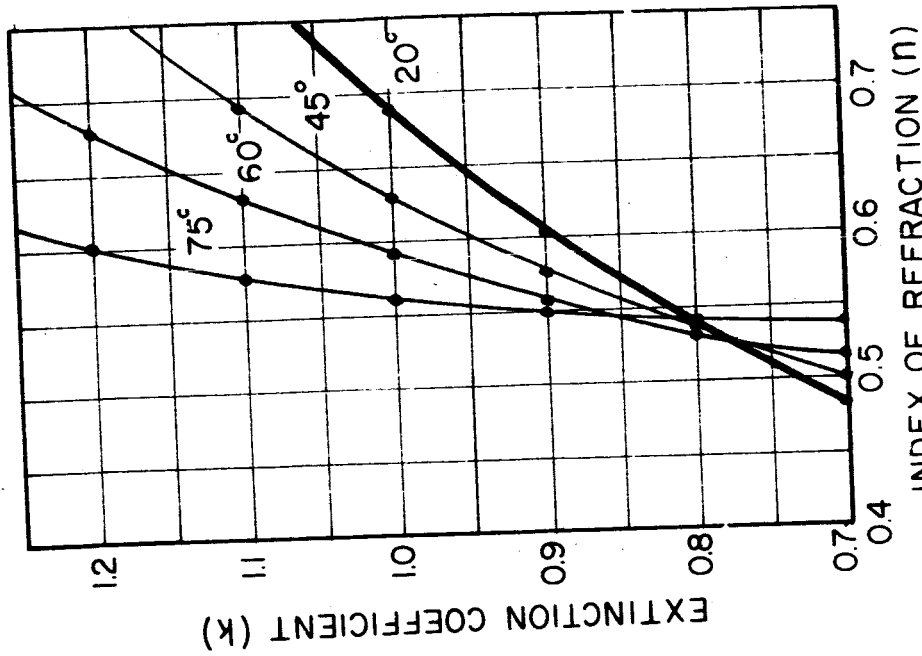
## FIGURE CAPTIONS

1. The calculation of optical constants by the reflectance method.
2. Reflectance vs angle of incidence curves calculated using the optical constants shown by the large numbers. For example, the lower left hand square shows  $R$  vs  $\phi$  curves for  $n = 0.3$  and  $k = 0.3$ .
3. Isorefectance curves for  $R_s$  calculated using the optical constants shown by the large numbers. The small numbers used for abscissa and ordinate show the scale in the  $n - k$  plane, and the numeral 8 designates the isorefectance curve corresponding to  $80^\circ$ . The other curves are for angles of incidence of  $70^\circ$ ,  $60^\circ$ , etc., through  $10^\circ$  and occur in descending order.
4. Isorefectance curves for  $R_p$  calculated using the optical constants shown by the large numbers. The small numbers used for abscissa and ordinate show the scale in the  $n - k$  plane, and the numeral 8 designates the isorefectance curve corresponding to  $80^\circ$ . The other curves are for angles of incidence of  $70^\circ$ ,  $60^\circ$ , etc., through  $10^\circ$  and, unless shown otherwise, occur in descending order.
5. Isorefectance curves for  $R_a$  calculated using the optical constants shown by the large numbers. The small numbers used for abscissa and ordinate show the scale in the  $n - k$  plane, and the numeral 8 designates the isorefectance curve corresponding to  $80^\circ$ . The other curves are for angles of incidence of  $70^\circ$ ,  $60^\circ$ , etc., through  $10^\circ$  and occur in descending order.

6. The effect of errors in reflectance measurements on an intersection of isorefectance curves. The angles of incidence are  $20^{\circ}$  and  $70^{\circ}$ .
7. The effect of non-parallelism of the incident radiation on the determination of  $n$  and  $k$ . The angles of incidence are  $20^{\circ}$  and  $70^{\circ}$ , and the divergence of the radiation is  $4^{\circ}$ .
8. The effect of  $\pm 1\%$  error in the measurement of reflectance on the determination of  $n$  and  $k$ . The angles of incidence are  $20^{\circ}$  and  $70^{\circ}$ .
9. The effect of polarization of the incident radiation used to measure  $R_a$  on the determination of  $n$  and  $k$ . The angles of incidence are  $20^{\circ}$  and  $70^{\circ}$ , the solid lines designate  $\pm 1\%$  polarization and the dotted lines  $\pm 5\%$  polarization.
10. Illustration of a scheme for digital computation of  $n$  and  $k$  from reflectance data.
11. Illustration of a scheme for tracing isorefectance curves using a digital computer-plotter combination.



CURVES SHOWING R AS A FUNCTION OF  $n$  FOR CONSTANT VALUES OF  $k$



CURVES OF CONSTANT REFLECTANCE FOR FOUR ANGLES OF INCIDENCE

# CALCULATION OF OPTICAL CONSTANTS BY THE REFLECTANCE METHOD

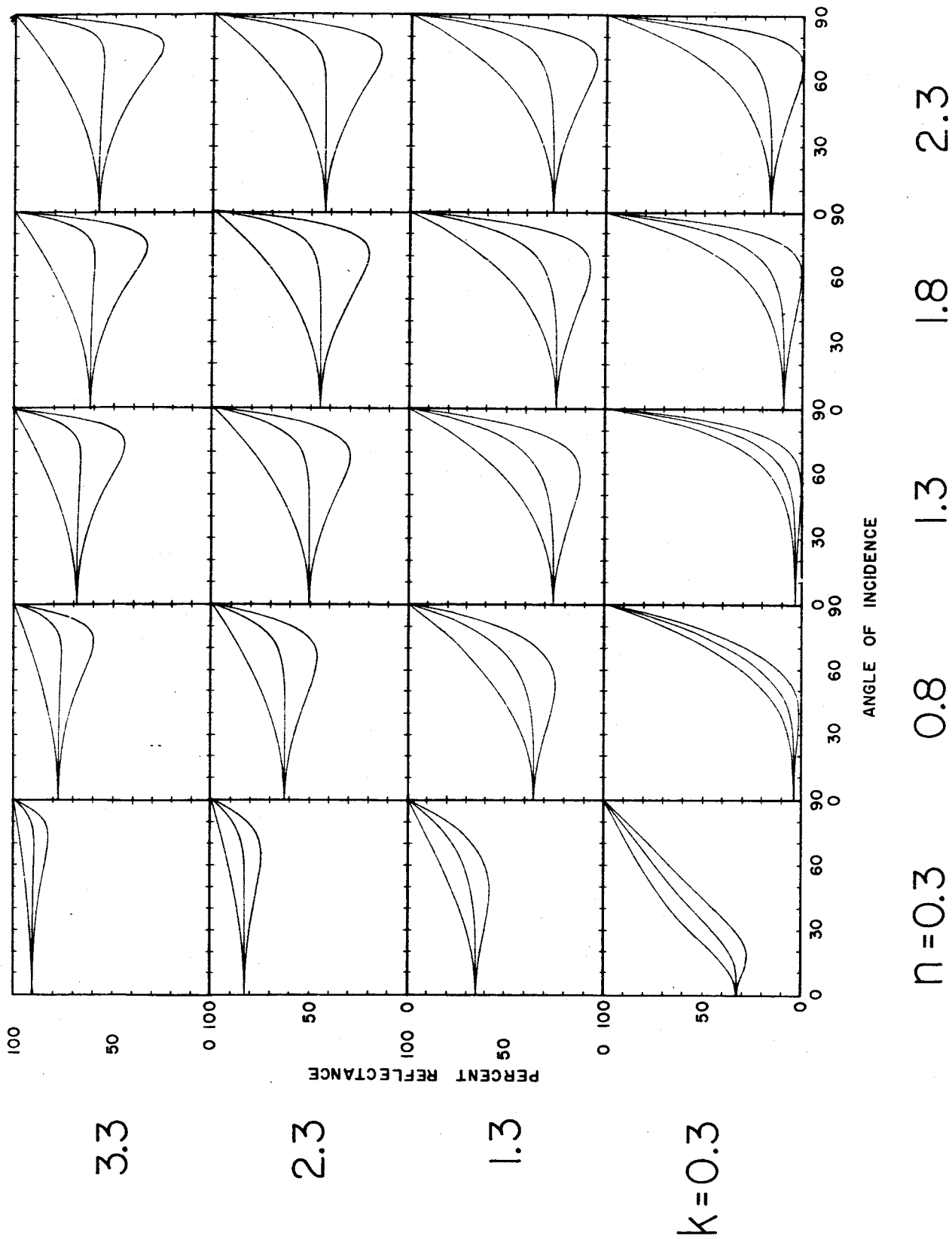


Fig. 2

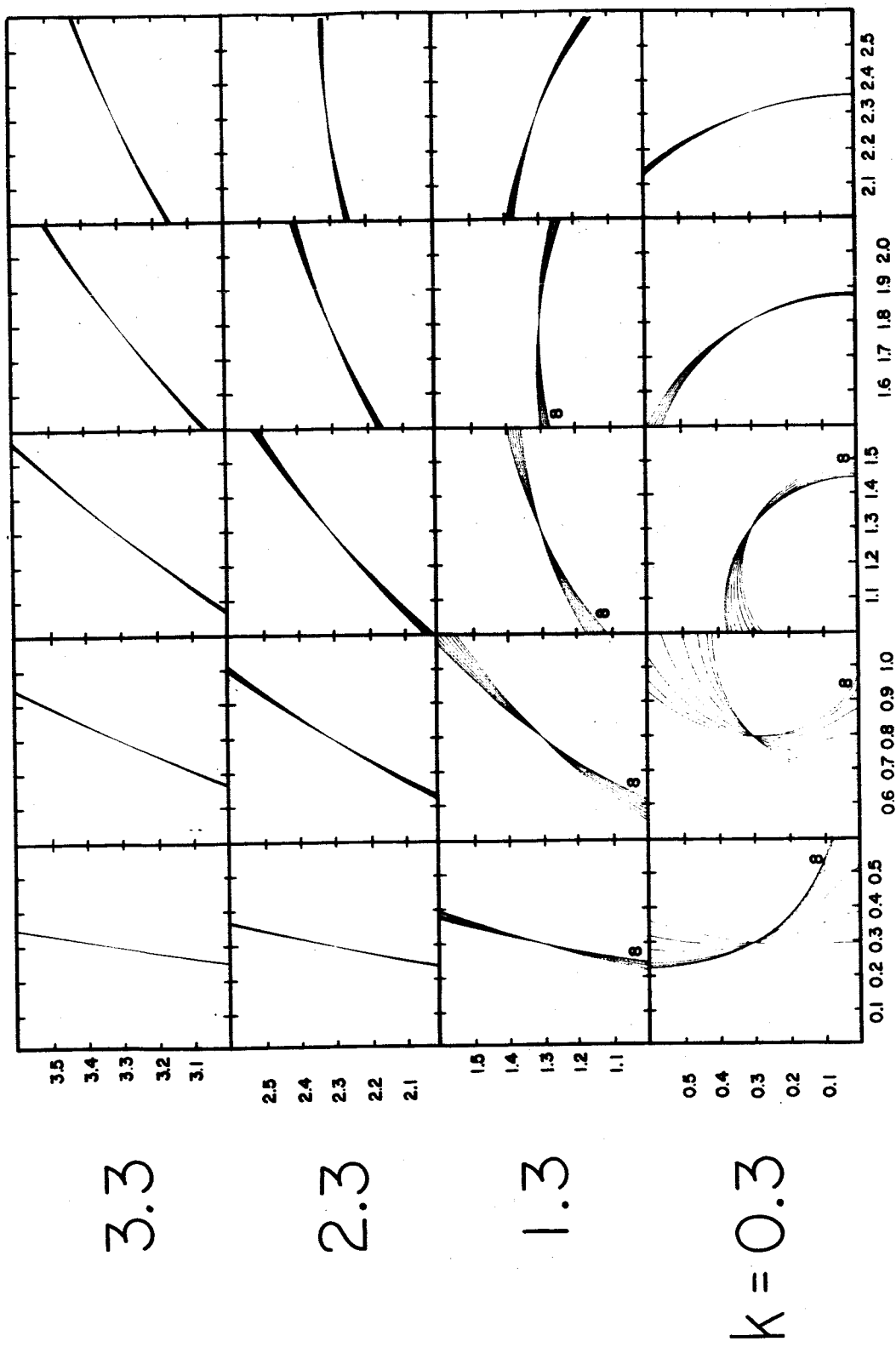
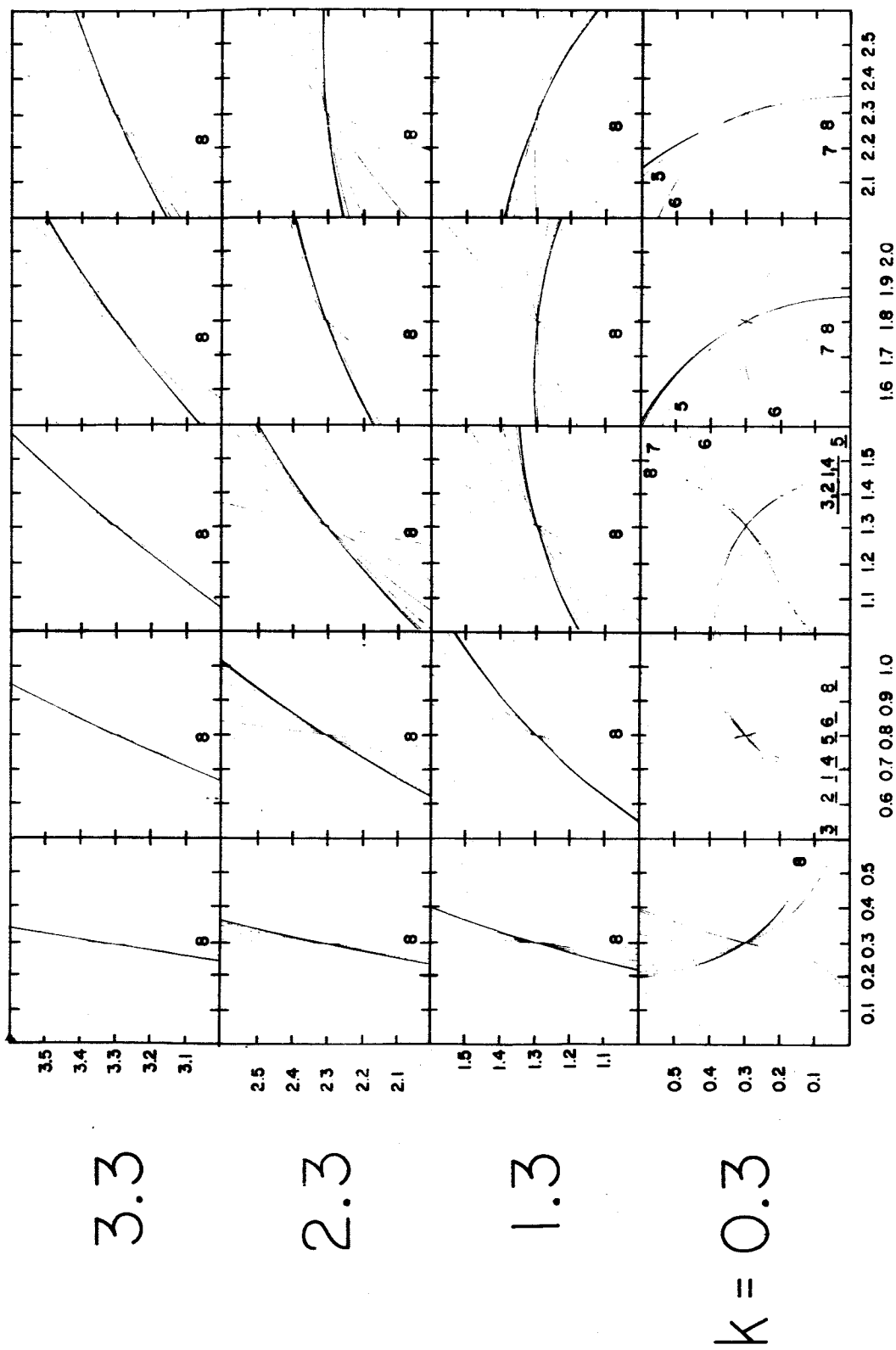


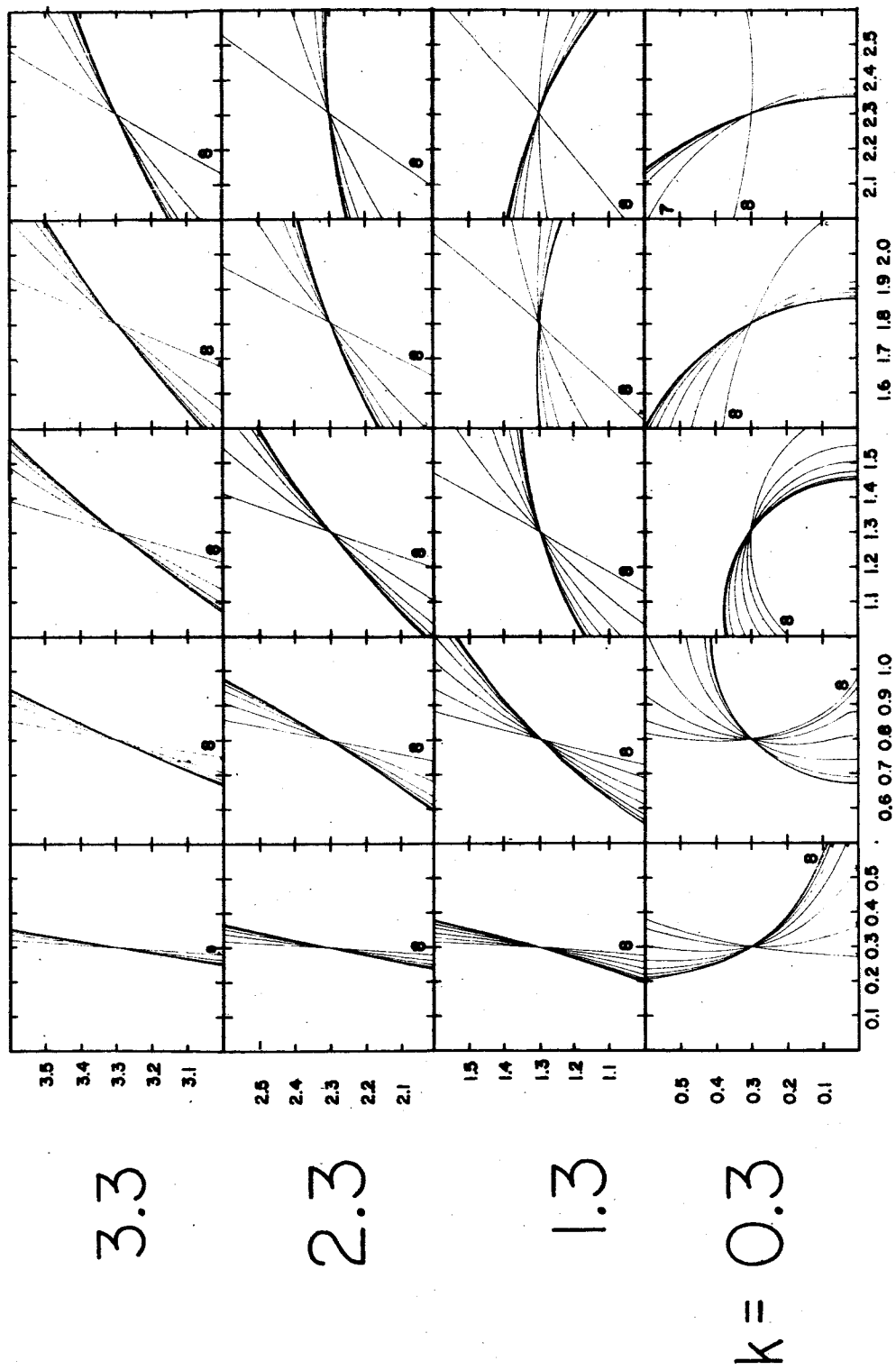
Fig. 3



$n = 0.3 \quad 0.8 \quad 1.3 \quad 1.8 \quad 2.3$

ISOREFLECTANCE CURVES FOR  $R_p$

Fig. 4

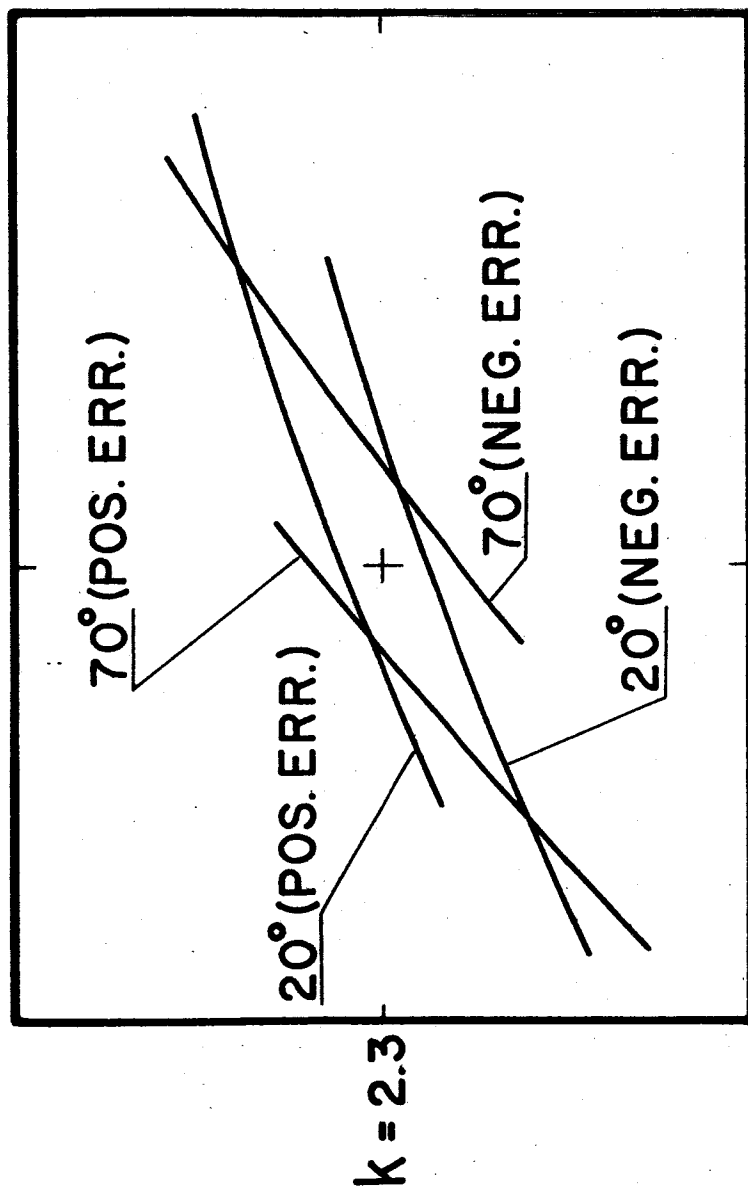


$n = 0.3 \quad 0.8 \quad 1.3 \quad 1.8 \quad 2.3$

ISOREFLECTANCE CURVES FOR  $(R_s + R_p)/2$

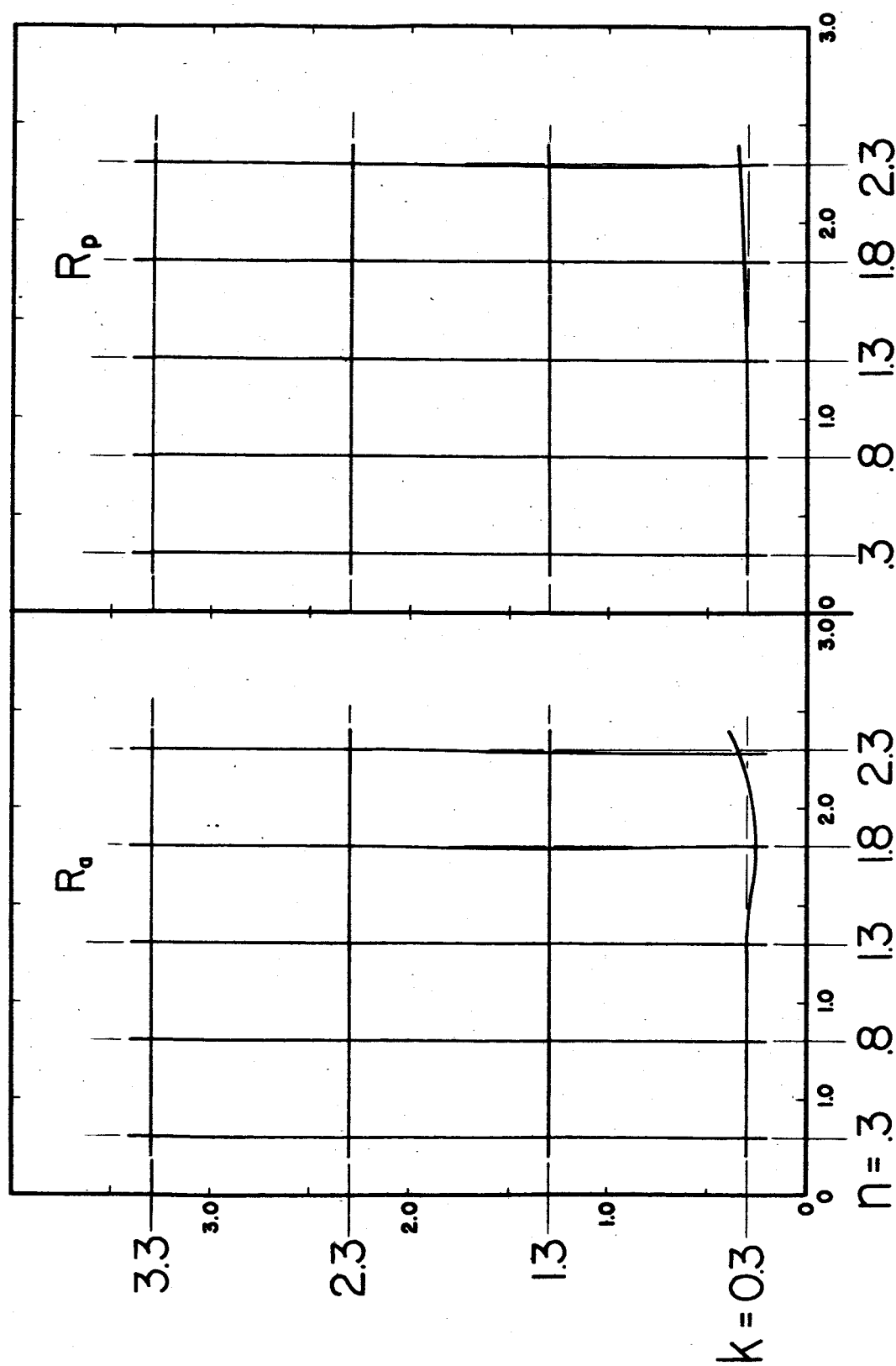
Fig. 5



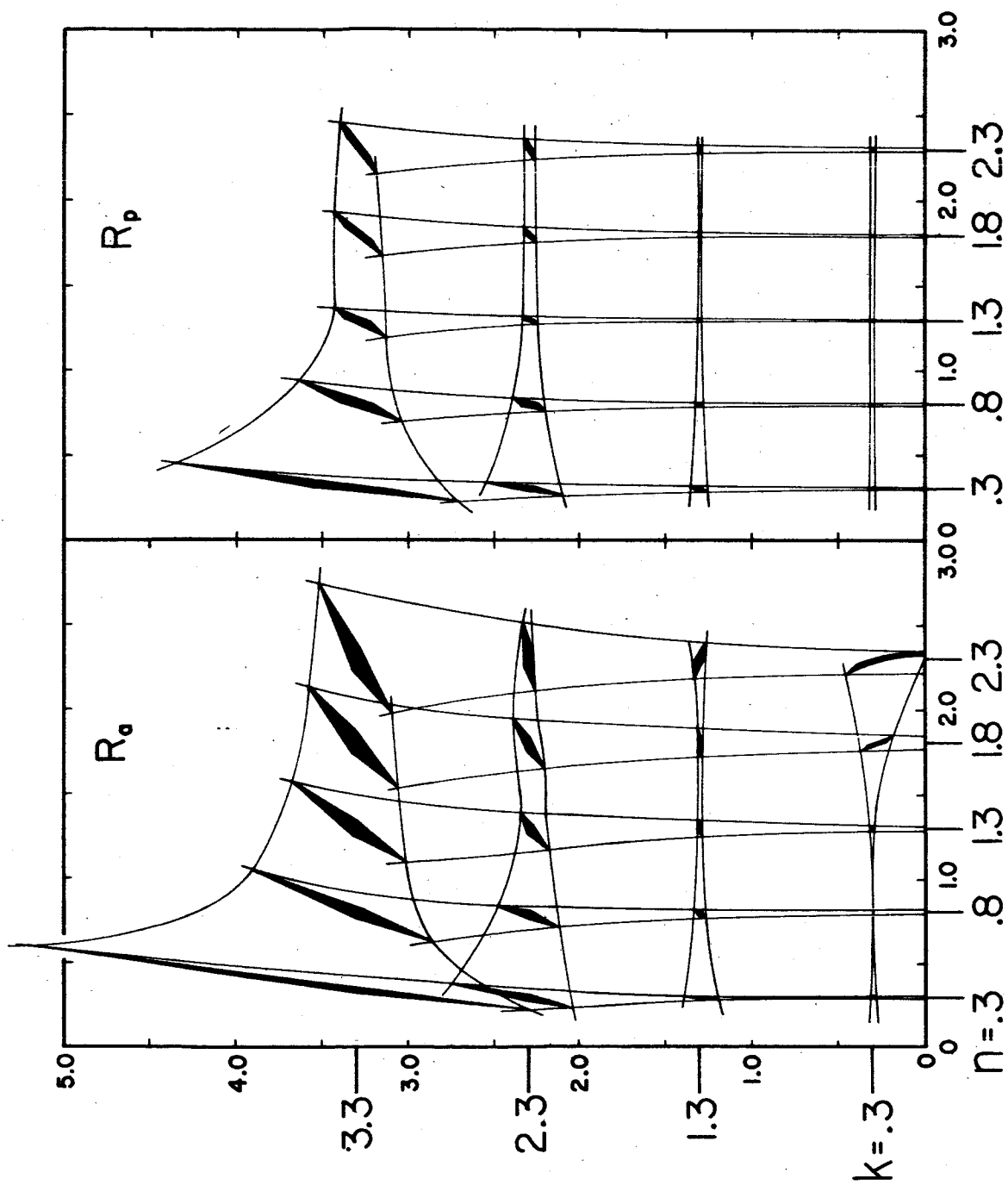


$n = 1.8$

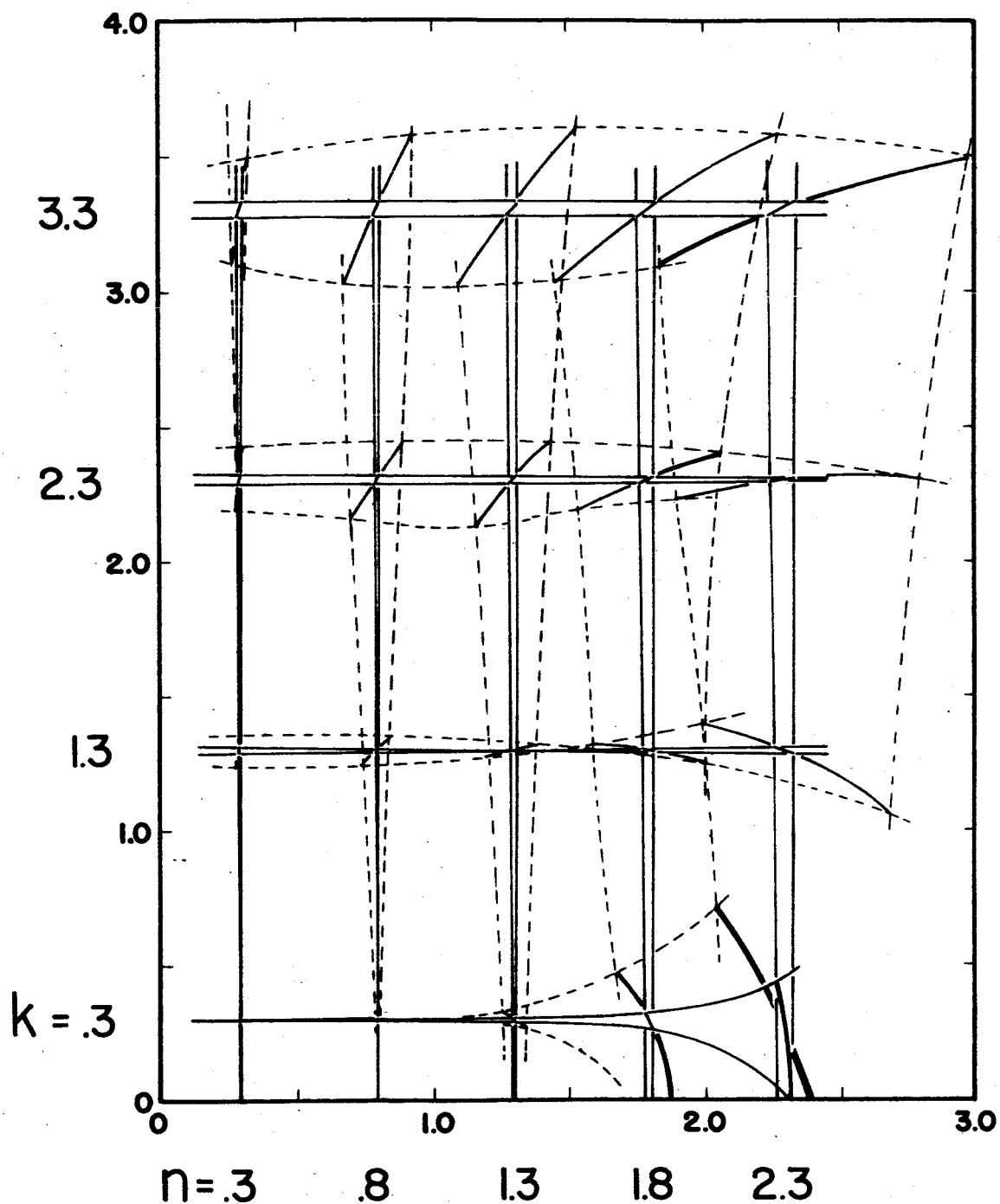
EFFECT OF ERRORS IN REFLECTANCE MEAS.  
ON INTERSECTION OF ISOREFLECTANCE CURVES



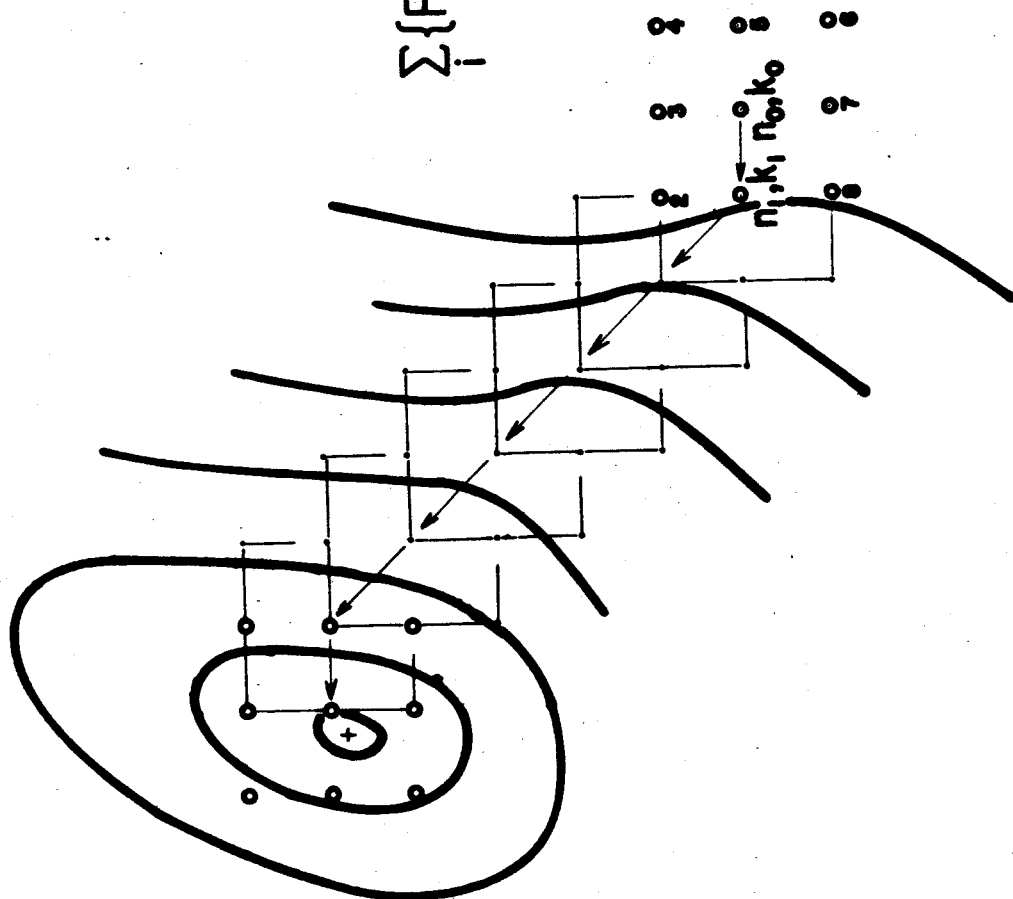
EFFECT OF NON-PARALLELISM OF INCIDENT RADIATION ON  
 DETERMINATION OF  $\eta$  &  $k$ . ANGLE OF INC.  $20^\circ$  &  $70^\circ$ ; DI-  
 VERGENCE OF INC. RADIATION,  $4^\circ$ .



EFFECT OF  $\pm 1\%$  ERROR IN MEASUREMENT OF REFLECTANCE ON DETERMINATION OF  $n$  &  $k$ . ANGLE OF INC.  $20^\circ$  &  $70^\circ$ .



EFFECT OF POLARIZATION OF INCIDENT RADIATION ON DETERMINATION OF  $n$  &  $k$ .  
 ANGLE OF INC.  $20^\circ$  &  $70^\circ$ . —  $\pm 1\%$ , ----  $\pm 5\%$ .



$$\sum_i \{R_{\text{meas.}}(\phi_i, n, k, p) - R_{\text{calc.}}(\phi_i, n_j, k_j, p)\}^2$$

$$= M_j(p)$$

Fig. 10

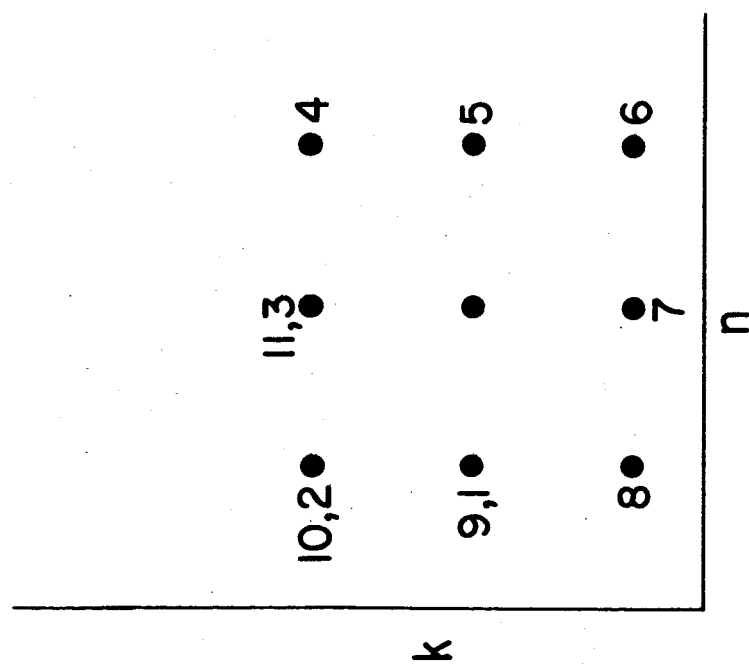
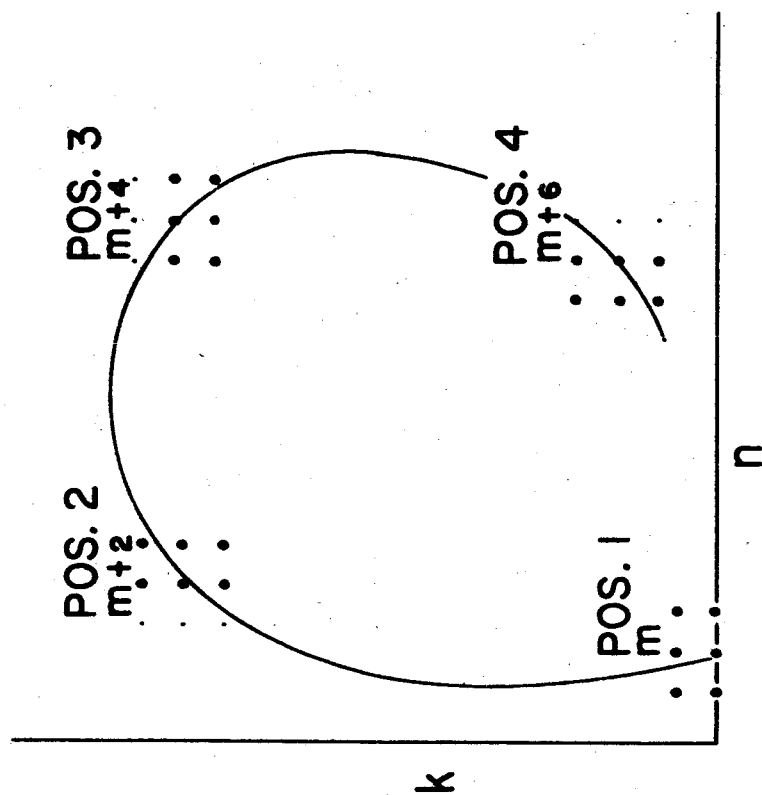


Fig. 11